

# Assessment of the efficiency of a pre- versus post-acquisition metal artifact reduction algorithm in the presence of 3 different dental implant materials using multiple CBCT settings: An in vitro study

Solaleh Shahmirzadi<sup>1,\*</sup>, Rana A. Sharaf<sup>2</sup>, Sarang Saadat<sup>3</sup>, William S. Moore<sup>2</sup>, Hassem Geha<sup>2</sup>, Dania Tamimi<sup>4</sup>, Husniye Demirturk Kocasarac<sup>5</sup>

<sup>1</sup>Department of Diagnostic Sciences, Division of Oral and Maxillofacial Radiology, Texas A&M College of Dentistry, Dallas, TX, USA

<sup>2</sup>Department of Comprehensive Dentistry, Division of Oral and Maxillofacial Radiology, University of Texas Health Science Center, San Antonio, TX, USA

<sup>3</sup>Department of Oral and Maxillofacial Surgery, University of Texas Health Science Center, San Antonio, TX, USA

<sup>4</sup>Private Practice, Oral and Maxillofacial Radiology, Orlando, FL, USA

<sup>5</sup>Department of General Dental Sciences, Division of Oral and Maxillofacial Radiology, Marquette University School of Dentistry, Milwaukee, WI, USA

## ABSTRACT

**Purpose:** The aim of this study was to assess artifacts generated in cone-beam computed tomography (CBCT) of 3 types of dental implants using 3 metal artifact reduction (MAR) algorithm conditions (pre-acquisition MAR, post-acquisition MAR, and no MAR), and 2 peak kilovoltage (kVp) settings.

**Materials and Methods:** Titanium-zirconium, titanium, and zirconium alloy implants were placed in a dry mandible. CBCT images were acquired using 84 and 90 kVp and at normal resolution for all 3 MAR conditions. The images were analyzed using ImageJ software (National Institutes of Health, Bethesda, MD) to calculate the intensity of artifacts for each combination of material and settings. A 3-factor analysis of variance model with up to 3-way interactions was used to determine whether there was a statistically significant difference in the mean intensity of artifacts associated with each factor.

**Results:** The analysis of all 3 MAR conditions showed that using no MAR resulted in substantially more severe artifacts than either of the 2 MAR algorithms for the 3 implant materials; however, there were no significant differences between pre- and post-acquisition MAR. The 90 kVp setting generated less intense artifacts on average than the 84 kVp setting. The titanium-zirconium alloy generated significantly less intense artifacts than zirconium. Titanium generated artifacts at an intermediate level relative to the other 2 implant materials, but was not statistically significantly different from either.

**Conclusion:** This in vitro study suggests that artifacts can be minimized by using a titanium-zirconium alloy at the 90 kVp setting, with either MAR setting. (*Imaging Sci Dent 2021; 51: 1-7*)

**KEY WORDS:** Cone-Beam Computed Tomography; Artifacts; Dental Implants

## Introduction

Imaging has become essential for implant dentistry planning and follow-up to monitor osseointegration and the out-

come of the bone integration process. Cone-beam computed tomography (CBCT) is currently one of the most commonly used techniques for the follow-up of bone integration around the dental implant due to its ability to provide precise 3-dimensional images.<sup>1</sup> These images have brought tremendous benefits in some dental specialties, such as periodontology, dental implantology, and oral and maxillofacial surgery.<sup>2,3</sup> One of the most important limitations of CBCT,

Received April 25, 2020; Revised November 24, 2020; Accepted November 25, 2020

\*Correspondence to : Dr. Solaleh Shahmirzadi

Department of Diagnostic Sciences, Division of Oral and Maxillofacial Radiology, Texas A&M College of Dentistry, 3302 Gaston Ave, Dallas, TX 75246, USA  
Tel) 1-615-927-9640, E-mail) s.shahmirzadi@tamu.edu

Copyright © 2021 by Korean Academy of Oral and Maxillofacial Radiology

This is an Open Access article distributed under the terms of the Creative Commons Attribution Non-Commercial License (<http://creativecommons.org/licenses/by-nc/3.0>) which permits unrestricted non-commercial use, distribution, and reproduction in any medium, provided the original work is properly cited.

Imaging Science in Dentistry · pISSN 2233-7822 eISSN 2233-7830

however, is its susceptibility to artifact generation.<sup>4</sup> Metallic objects significantly deteriorate CBCT image quality due to scattering, beam hardening, and streak artifacts that hinder the proper visualization of peri-implant bone and osseointegration,<sup>5</sup> thereby making the diagnosis ineffectual and time-consuming.<sup>6</sup>

Significant efforts have been made to develop metal artifact reduction (MAR) algorithms to reduce beam hardening effects and improve CBCT scan quality. Some CBCT machines have the option of applying a pre- or post-acquisition MAR algorithm, which is a newly introduced type of software that can reduce artifacts and enhance the quality of images produced. Pre- and post-acquisition MAR is based on standardizing voxel values by enhancing the reconstruction of the image and improving the contrast-to-noise ratio (CNR) to diminish the deleterious impacts of artifacts.<sup>7</sup> The pre-acquisition MAR algorithm identifies the metal area in the basis projections. The metal projection data are then processed with the interpolation algorithm. Finally, CT axial images are reconstructed from the pre-processed data sets, and the metal section is recovered.<sup>8</sup> In the post-acquisition algorithm, metal regions in each projection are segmented and modified. The reconstruction of the final CT image with the modified data is displayed. Nevertheless, due to the proximity of the voxel values of bone and metal, it is difficult to develop an algorithm for accurate metal segmentation.<sup>8</sup> Additionally, different peak tube potentials (peak kilovoltage; kVp) can be applied to reduce metal artifacts.<sup>9</sup>

Various materials, such as titanium-zirconium (Ti-Zr), titanium (Ti), and zirconium dioxide (ZrO<sub>2</sub>), are increasingly being used to manufacture implants with enhanced mechanical properties. For decades, Ti has been used to manufacture dental implants due to its ideal properties and favorable ability to osseointegrate.<sup>10</sup> ZrO<sub>2</sub> then emerged as an alternative to overcome some limitations of Ti, such as an esthetically unfavorable appearance and artifact generation,<sup>11</sup> and the overall survival rate of zirconia implants has been calculated as 92% (95% CI, 87-95) after 1 year of function.<sup>12</sup> Alloying elements can be also added to Ti to improve its characteristics.<sup>13</sup> Ti-Zr implants were recently introduced for clinical applications, and the mean survival and success rates of Ti-Zr implants have been reported as 98.4% and 97.8% at 1 year after implant placement and 97.7% and 97.3% at 2 years, respectively.<sup>14</sup> To date, insufficient information has been made available to compare artifacts due to these 3 different types of implants in CBCT scans using pre- and post-acquisition MAR, as compared to images without MAR. Therefore, it is necessary to investi-

gate the difference in artifacts induced by Ti-Zr, Ti, and ZrO<sub>2</sub> implants in CBCT scans.

The objective of this study was thus to evaluate and compare the effects of pre- and post-acquisition MAR on artifacts produced by 3 common types of implant materials at 2 different kVp settings, to determine whether they have the intended effect (artifact reduction relative to images taken without the MAR algorithm) and whether any method is better than another for any of the implant metals.

## Materials and Methods

### Implant phantoms

Three types of implant materials were used for this study: titanium-zirconium (Ti-ZrO<sub>2</sub>; Roxolid, Straumann, Basel, Switzerland) with dimensions of 4.1 mm (diameter) × 8 mm (length), titanium grade 4 (Ti; BEGO Semados Implants, BEGO Implant Systems GmbH & Co. KG, Bremen, Germany) with dimensions of 4.1 mm (diameter) × 10 mm (length), and zirconium (ZrO<sub>2</sub>; PURE Ceramic Implant, Straumann, Basel, Switzerland) with dimensions of 4.1 mm (diameter) × 16 mm (length).

The implant samples were placed in a dried human mandibular premolar socket. An epoxy resin-based substitute was placed on the contralateral side in contact with the lingual aspect of the mid-height of the mandibular molar region to provide a homogeneous control area. A control area was chosen that would be unaffected, or minimally affected, by the artifacts generated by the implants. The phantom was fixed at the floor of the container filled with water, while the occlusal plane was parallel to the horizontal plane. The study model was placed in the center of the field of view (FOV) by applying the laser orientation beams.

### CBCT scanning

CBCT images were acquired for each type of implant using a Planmeca CBCT machine (ProMax<sup>®</sup> 3D Max; Planmeca, Helsinki, Finland) with the following parameters: normal resolution, FOV of 8 × 8 cm, 84 kVp or 90 kVp, with pre- and post-acquisition medium MAR or no MAR. These are the most often used parameters for implant imaging in our clinic. The images were obtained at 8 mA, with a 200- $\mu$ m voxel size and an exposure time of about 12 seconds.

The position of the mandible within the chosen FOV was similar for all scans. The acquisitions were repeated 5 times for each setting to measure variance in artifacts within a specific modality. For comparative purposes, the extent of artifacts was measured for all 3 MAR conditions and both kVp levels without an implant as well. Therefore, 30 scans

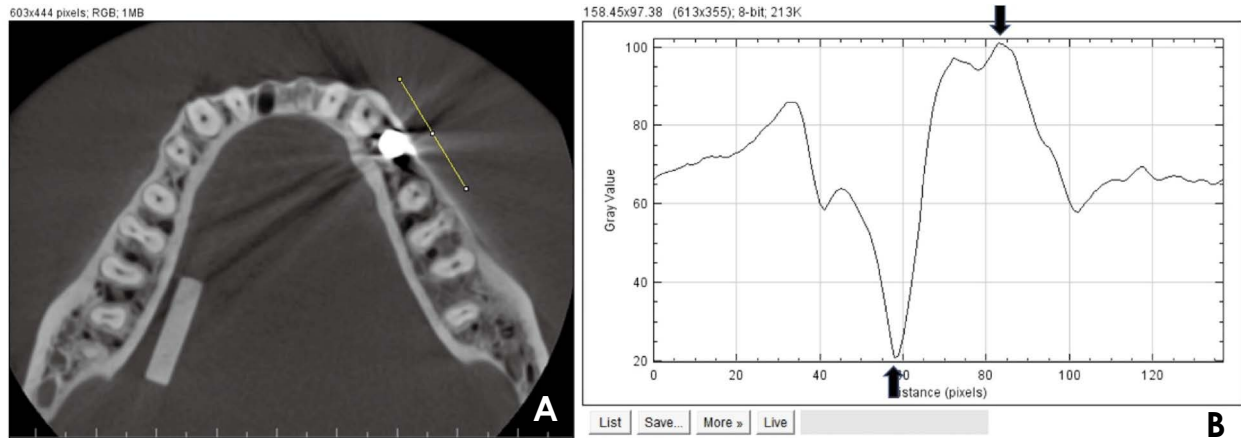


**Fig. 1.** A. A profile line is plotted in the water adjacent to the implant, crossing through the streaking and beam-hardening artifacts. B. The difference between the highest (top arrow) and lowest (bottom arrow) gray values is calculated and referred to as the artifact intensity value.

were acquired for each type of implant, and a total of 120 images with and without implants were evaluated.

#### CBCT image evaluation

After the acquisition of the scans, volumetric data were reconstructed and exported to the Digital Imaging and Communications in Medicine file format with a 0.2-mm thickness. Axial reconstructions were used for data assessment. A specified axial slice (slice #297) was chosen as the best representative of the artifacts and used for all the scans taken to ensure consistency among all scans. Due to the exact repositioning of the phantom in the machine, all the evaluated slices were identical. The images were then analyzed using ImageJ software (ImageJ 1.52a, National Institutes of Health, Bethesda, MD, <https://imagej.nih.gov/ij/>) to calculate the intensity of artifacts that resulted from each implant material. A plot profile line was used to analyze voxel value variation in the images. The line was placed through the beam-hardening dark bands and straight lines of streaking artifacts. In all analyses, the lines had the same length and the same distance from the implant bodies. The voxel value at the lowest peak was then subtracted from the highest peak and the difference was used to quantify the intensity of artifacts in each scan (Figs. 1A and B).

#### Statistical analysis

The artifacts measured for each image were first evaluated to verify that the 2 types of MAR (pre- and post-acquisition) were better than using no MAR at all. Then the mean and standard deviation of artifact values were compared across the 3 types of implants without the MAR setting to visualize the effect of each type of metal on artifact production. Finally, artifacts were compared with the 2 modes of MAR at

the 2 kVp settings (84 kVp or 90 kVp) and the 3 types of implant to determine whether any mode of MAR was better than another at artifact reduction, and whether the kVp setting or type of material made a difference on the effect of MAR mode. The R statistical package (R version 3.6.3, R Core Team (2020). R: A language and environment for statistical computing. R Foundation for Statistical Computing, Vienna, Austria, [www.R-project.org](http://www.R-project.org)) was used for the statistical computations. Analysis of variance (ANOVA) was used as a general linear model to make statistical comparisons, with MAR setting, type of implant, and kVp setting as the factors, and allowing for the possibility of up to 3-way interactions. The Tukey honest significant difference (HSD) test was used *post hoc* to determine which type of implant resulted in the least intense artifacts. *P*-values < 0.05 were taken to indicate statistical significance.

## Results

The intensity of artifacts generated when there was no metal implant material was measured to establish a baseline for comparison with the artifacts generated by implant materials. With no MAR setting, the intensity of the artifacts generated under the conditions of this experiment was 168 at 84 kVp and 172 at 90 kVp. The values for the artifacts using post-acquisition MAR were essentially the same: 169 at 84 kVp and 172 at 90 kVp. For pre-acquisition MAR, slightly higher values were observed (221 at 84 kVp and 200 at 90 kVp). Although the intensity of the artifacts was measured 5 times for each condition, there was no variation in the artifact intensity measurement within any of the 6 conditions.

When the implant materials were imaged, the mean value

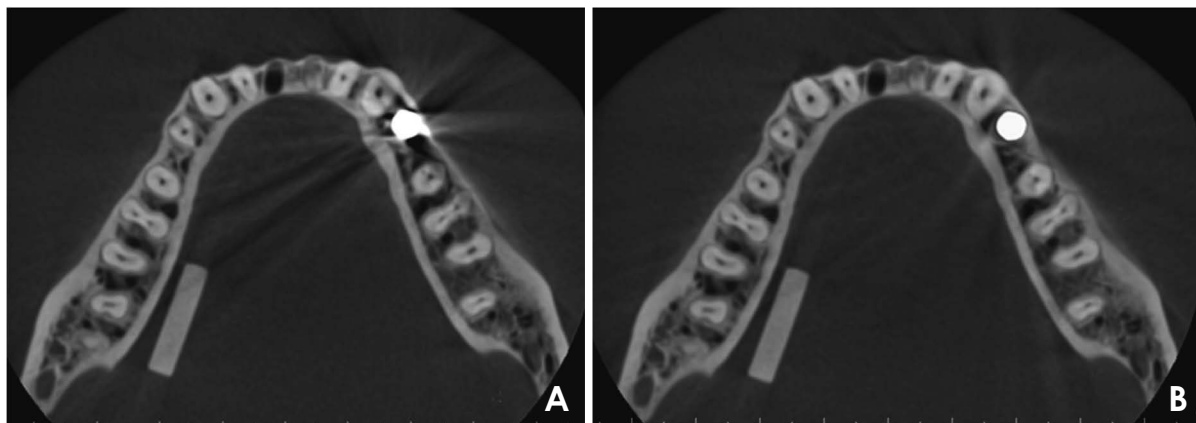


**Fig. 2.** Example of axial images shows the efficacy of the metal artifact reduction (MAR) algorithm. A. 84 kVp and no MAR. B. 84 kVp and pre-acquisition MAR.

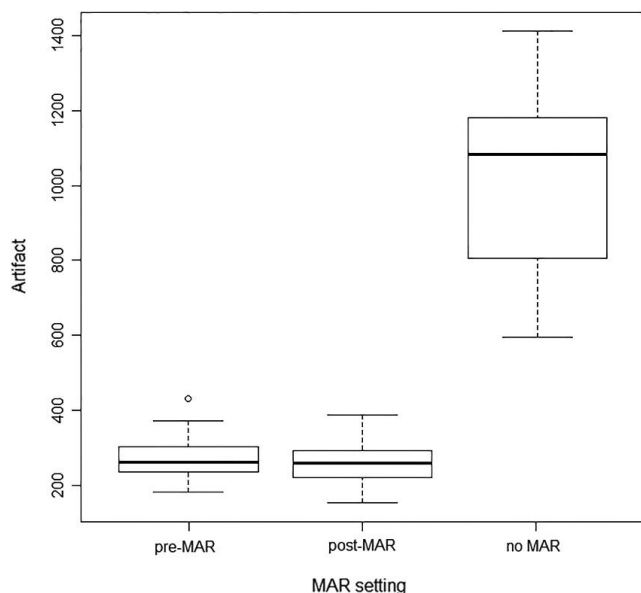


**Fig. 3.** Box plots of artifacts associated with metal artifact reduction (MAR) settings, showing the aggregation across all materials and kVp settings. The whiskers of each boxplot show the minimum and maximum values within each data set, the thick middle line is the median value, and the bottom and top of the boxes are the first and third quartiles, which indicate where the middle 50% of the data lie.

of artifact intensity with no MAR (across all 6 combinations of materials and kVp settings) was 1005, while the mean value of artifact intensity with either setting of MAR was 268, reflecting a statistically significant difference ( $P < 0.05$ ) (Fig. 2). The difference in mean values can readily be seen in the boxplots in Figure 3. To confirm the efficacy of the MAR algorithms, the data were divided into 2 sets: images obtained with no MAR, versus images obtained with either of the 2 MAR settings. Boxplots of the artifact data from the

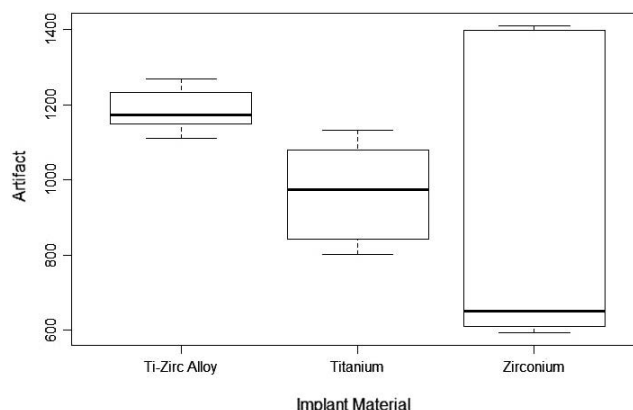


**Fig. 4.** Box plots of artifacts by implant material aggregated across all metal artifact reduction (MAR) and kVp settings.

no-MAR images are shown in Figure 4 to assist in visualizing how the implant material affected artifacts. The Ti-Zr images had the highest median level of artifacts, but the least amount of variability, whereas the images with  $ZrO_2$  as the implant material had the lowest median amount of artifacts, but an extreme amount of variability. The Ti material had moderate levels of both artifact intensity and variability.

With the data from no-MAR setting removed, the 3-factor ANOVA indicated no detectable difference in artifacts between the 2 remaining MAR settings ( $P = 0.25$ ), but a statistically significant difference in the artifacts generated between at least 2 implant materials ( $P < 0.05$ ) and between the 2 kVp settings ( $P < 0.05$ ). No interaction term was significant. The 90 kVp setting generated less intense artifacts on average than the 84 kVp setting. The Tukey HSD test indicated that with the MAR setting on, the Ti-Zr alloy gen-

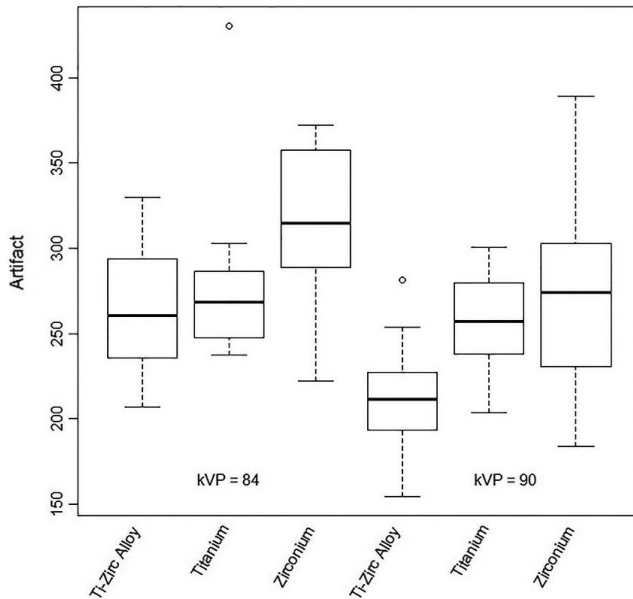


**Fig. 5.** Box plots of artifacts by implant material and kVp setting aggregated across the pre- and post-acquisition MAR settings

erated significantly less intense artifacts than the  $ZrO_2$  alloy ( $P < 0.05$ ). The mean intensity of artifacts generated by Ti fell between the other 2 implant materials, but was not statistically different from either.

Figure 5 illustrates the distribution of artifact intensity across the 6 combinations of implant materials and kVp settings, aggregated across the MAR setting, to assist in visualizing the artifacts for each modality. This demonstrates that the 90 kVp setting resulted in a less intense artifacts and that Ti-Zr generated less intense artifacts than  $ZrO_2$ . These findings also suggest that artifacts can be minimized by using the Ti-Zr alloy at the 90 kVp setting, with either MAR setting.

## Discussion

Conventional CT has limited value compared to CBCT for assessing the peri-implant bone tissue, and there has been an increasing interest in applying CBCT to evaluate osseointegration around implants.<sup>2</sup> However, the main shortcoming of CBCT is the appearance of dark areas around high-density materials that cause less reliable interpretation of images. Therefore, MAR algorithms have been added into CBCT machines to correct artifacts.

According to the results of previous studies, the MAR algorithm increases the CNR and decreases the noise when there is a high-density material within the FOV. However, Vasconcelos et al. reported that the CNR was systematically better when they did not use the MAR algorithm for

$ZrO_2$  implants.<sup>3</sup> Similar results were shown by Bezerra et al.,<sup>15</sup> who reported that CNR was reduced by applying the MAR algorithm when there were metal posts within the FOV. In addition, some other studies reported that the MAR tool may neither improve the voxel values nor eliminate artifacts entirely.<sup>3</sup> Therefore, MAR may not generate a more precise scan. Nevertheless, Bechara et al. showed that applying MAR resulted in a higher CNR and a significant change in mean voxel levels when metal was present in the FOV.<sup>9</sup> These findings are in concordance with the findings of Demirturk Kocasarac et al.<sup>16</sup> Those authors used the MAR algorithm in the presence of 4 different types of root end filling materials and showed that MAR markedly minimized the metal artifacts and increased the CNR, suggesting that it improved image quality.<sup>16</sup>

Possible reasons for the contrasting findings among the abovementioned studies may be that some of the previous authors used the CNR to evaluate image changes. Instead, this study used a line profile measurement in the area of interest next to the implant. The line profile provides a linear measurement of the difference between the highest and lowest gray values, and not overall image quality. The CNR is one of the main factors influencing the image quality in CBCT, but was not within the scope of this study. In addition, decreased artifact values are seen when MAR is used, but how the images might look without the implant material in the FOV is unknown. Therefore, it is unclear whether the parameters used or MAR algorithm application actually restore the image content to offer a closer demonstration of the underlying reality (e.g., whether the adjusted image represents the actual object attenuation better than the non-adjusted image, or whether these settings are all merely a matter of iteration or interpolation aiming to decreasing the influence of the high-attenuating materials). The gray values attained by using the MAR algorithm might be different from those that would be computed if the same image were obtained with no metal in the FOV.<sup>7</sup> Nonetheless, besides all its advantages, the reconstruction time is longer when the MAR algorithm is applied.<sup>17</sup>

Bechara et al.<sup>17</sup> found that the quality of scans was better when applying pre-acquisition MAR, rather than post-acquisition MAR, when they evaluated the effect of the MAR algorithm in the proximity of a metallic bead. In contrast, Bechara et al.<sup>6</sup> suggested using post-processing MAR when they investigated the effect of the MAR algorithm on the detection of root fractures. In another study done using the Planmeca ProMax device, Kamburoglu et al.<sup>18</sup> did not find a statistically significant difference in the discernment of peri-implant bone defects with and without use of the

MAR algorithm. Although pre- and post-processing MAR may improve CBCT images by minimizing metal artifacts, there are always some missed data that cannot be recreated.<sup>18,19</sup>

Based on our findings, with the no-MAR setting, considerable artifacts were generated due to dental implant materials. However, there was no detectable difference in artifact intensity between the 2 MAR settings (pre- and post-acquisition).

It has been stated that the amount of artifact generation in CT/CBCT has a relationship with the atomic number of the element. Sancho-Puchades et al.<sup>4</sup> determined that ZrO<sub>2</sub> implants produced the most artifacts in CBCT images, followed by Ti-Zr and Ti implants, and Pekkan et al.<sup>20</sup> found that the radiopacity of ZrO<sub>2</sub> was more than twice as high as that of Ti. The radiopacity of a material is based on multiple factors such as atomic number, shape, dimension, density, and some other physical attributes. Of these factors, the atomic number (Z) of an element is the factor with the highest impact on its opacity. An element with a greater atomic number produces more artifacts.<sup>4</sup> Thus, the differences in the severity of artifacts in CBCT images of Ti-Zr, Ti, and ZrO<sub>2</sub> can be explained by differences in their atomic numbers: titanium (Z: 22), zirconium (Z: 40), and oxygen (Z: 8).<sup>13</sup>

Despite the increased use of ceramic material due to its several advantages, such as tissue-friendliness, natural color, high bonding strength, and hardness, Demirturk Kocasarac et al.<sup>21</sup> showed that ZrO<sub>2</sub> implants underachieved in comparison with Ti and Ti-Zr implants because they generated more artifacts in CT and CBCT scans. Sancho-Puchades et al.<sup>4</sup> also stated that Ti implants generated less artifacts than ZrO<sub>2</sub> implants in CBCT images. The results of this study suggest that the Ti-Zr alloy generated less intense artifacts than the ZrO<sub>2</sub> alloy, while the artifacts generated by Ti were intermediate between the other 2 implant materials, but was not statistically significantly different from either.

Moreover, different kVp settings influence the intensity of artifacts in CBCT scans to a remarkable extent. Esmaeili et al. and Draenert et al. found that higher kVp settings created fewer artifacts. Higher kVp settings generate more energetic and numerous photons that hit the detectors, leading to fewer artifacts. Esmaeili et al.<sup>22</sup> compared dental implant-generated artifacts in 2 CBCT machines, while Draenert et al.<sup>23</sup> compared the dental implant-associated artifacts produced by CBCT and 4-row multi-detector CT. According to Schulze et al., the artifacts generated by dental implants were reduced by using higher kVp settings. However, Haramati et al.<sup>24</sup> obtained no advantage by using a high

kVp setting to refine the image quality around the metal prosthesis in CT scans. Nevertheless, our study showed that the higher kVp setting resulted in lower artifact intensity. Various methods have been used to reduce metal artifacts in different CBCT machines; however, further studies are needed to establish whether their application is clinically reliable for eliminating artifacts.

Despite efforts to properly place the implants within the machines and to use standard implant protocols to mimic in vivo conditions, the in vitro nature of this study was still a limitation. In vivo, the voxel value measurements are influenced by nearby anatomic structures, while the geometric distribution and intensity of artifacts for imaging techniques are only affected by the experimental setup in vitro. In actual clinical cases, several factors (e.g., patient movement during the scan, and metallic artifacts due to prostheses) might hinder the diagnosis. Other limitations are the limited sample size of 4 implants and the use of only 1 CBCT unit. Hence, future studies are needed for in vivo testing with different types of machines and a larger sample.

In conclusion, this in vitro study suggests that even though MAR decreased the intensity of image artifacts, no significant difference in terms of artifact generation was found according to whether the algorithm was applied before or after image acquisition. For instance, if the operator does not turn on the algorithm prior to acquisition for some reason, he/she can turn it on after image acquisition and still obtain the same amount of MAR. In addition, artifacts can be minimized by using a Ti-Zr alloy, in comparison to Ti and ZrO<sub>2</sub> alloys, at a high kVp setting.

**Conflicts of interest:** None

## References

1. Kamburoğlu K, Murat S, Kılıç C, Yüksel S, Avsever H, Farman A, et al. Accuracy of CBCT images in the assessment of buccal marginal alveolar peri-implant defects: effect of field of view. *Dentomaxillofac Radiol* 2014; 43: 20130332.
2. Scarfe WC, Farman AG, Sukovic P. Clinical applications of cone-beam computed tomography in dental practice. *J Can Dent Assoc* 2006; 72: 75-80.
3. Bechara B, McMahan CA, Moore WS, Noujeim M, Geha H. Contrast-to-noise ratio with different large volumes in a cone-beam computerized tomography machine: an in vitro study. *Oral Surg Oral Med Oral Pathol Oral Radiol* 2012; 114: 658-65.
4. Sancho-Puchades M, Hämmerle CH, Benic GI. In vitro assessment of artifacts induced by titanium, titanium-zirconium and zirconium dioxide implants in cone-beam computed tomography. *Clin Oral Implants Res* 2015; 26: 1222-8.

5. Angelopoulos C, Aghaloo T. Imaging technology in implant diagnosis. *Dent Clin North Am* 2011; 55: 141-58.
6. Bechara B, McMahan CA, Moore WS, Noujeim M, Teixeira FB, Geha H. Cone beam CT scans with and without artefact reduction in root fracture detection of endodontically treated teeth. *Dentomaxillofac Radiol* 2013; 42: 20120245.
7. Bechara B, Moore WS, McMahan CA, Noujeim M. Metal artefact reduction with cone beam CT: an in vitro study. *Dentomaxillofac Radiol* 2012; 41: 248-53.
8. Parsa A, Ibrahim N, Hassan B, Syriopoulos K, van der Stelt P. Assessment of metal artefact reduction around dental titanium implants in cone beam CT. *Dentomaxillofac Radiol* 2014; 43: 20140019.
9. Robertson DD, Weiss PJ, Fishman EK, Magid D, Walker PS. Evaluation of CT techniques for reducing artifacts in the presence of metallic orthopedic implants. *J Comput Assist Tomogr* 1988; 12: 236-41.
10. Wennerberg A, Albrektsson T. On implant surfaces: a review of current knowledge and opinions. *Int J Oral Maxillofac Implants* 2010; 25: 63-74.
11. Vasconcelos TV, Bechara BB, McMahan CA, Freitas DQ, Noujeim M. Evaluation of artifacts generated by zirconium implants in cone-beam computed tomography images. *Oral Surg Oral Med Oral Pathol Oral Radiol* 2017; 123: 265-72.
12. Hashim D, Cionca N, Courvoisier DS, Mombelli A. A systematic review of the clinical survival of zirconia implants. *Clin Oral Investig* 2016; 20: 1403-17.
13. Kobayashi E, Matsumoto S, Doi H, Yoneyama T, Hamanaka H. Mechanical properties of the binary titanium-zirconium alloys and their potential for biomedical materials. *J Biomed Mater Res* 1995; 29: 943-50.
14. Altuna P, Lucas-Taulé E, Gargallo-Albiol J, Figueras-Álvarez O, Hernández-Alfaro F, Nart J. Clinical evidence on titanium-zirconium dental implants: a systematic review and meta-analysis. *Int J Oral Maxillofac Surg* 2016; 45: 842-50.
15. Bezerra IS, Neves FS, Vasconcelos TV, Ambrosano GM, Freitas DQ. Influence of the artefact reduction algorithm of Picasso Trio CBCT system on the diagnosis of vertical root fractures in teeth with metal posts. *Dentomaxillofac Radiol* 2015; 44: 20140428.
16. Demirturk Kocasarac H, Helvacioğlu Yigit D, Bechara B, Sinanoglu A, Noujeim M. Contrast-to-noise ratio with different settings in a CBCT machine in presence of different root-end filling materials: an in vitro study. *Dentomaxillofac Radiol* 2016; 45: 20160012.
17. Bechara B, McMahan CA, Geha H, Noujeim M. Evaluation of a cone beam CT artefact reduction algorithm. *Dentomaxillofac Radiol* 2012; 41: 422-8.
18. Kamburoglu K, Kolsuz E, Murat S, Eren H, Yüksel S, Paksoy CS. Assessment of buccal marginal alveolar peri-implant and periodontal defects using a cone beam CT system with and without the application of metal artefact reduction mode. *Dentomaxillofac Radiol* 2013; 42: 20130176.
19. Schulze RK, Berndt D, d'Hoedt B. On cone-beam computed tomography artifacts induced by titanium implants. *Clin Oral Implants Res* 2010; 21: 100-7.
20. Pekkan G, Pekkan K, Hatipoglu MG, Tuna SH. Comparative radiopacity of ceramics and metals with human and bovine dental tissues. *J Prosthet Dent* 2011; 106: 109-17.
21. Demirturk Kocasarac H, Ustaoglu G, Bayrak S, Katkar R, Geha H, Deahl ST 2nd, et al. Evaluation of artifacts generated by titanium, zirconium, and titanium-zirconium alloy dental implants on MRI, CT, and CBCT images: a phantom study. *Oral Surg Oral Med Oral Pathol Oral Radiol* 2019; 127: 535-44.
22. Esmaeili F, Johari M, Haddadi P, Vatankhah M. Beam hardening artifacts: comparison between two cone beam computed tomography scanners. *J Dent Res Dent Clin Dent Prospects* 2012; 6: 49-53.
23. Draenert FG, Coppenrath E, Herzog P, Müller S, Mueller-Lisse UG. Beam hardening artefacts occur in dental implant scans with the NewTom cone beam CT but not with the dental 4- row multidetector CT. *Dentomaxillofac Radiol* 2007; 36: 198-203.
24. Haramati N, Staron RB, Mazel-Sperling K, Freeman K, Nickoloff EL, Barax C, et al. CT scans through metal scanning technique versus hardware composition. *Comput Med Imaging Graph* 1994; 18: 429-34.